Journal of Applied Polymer Science

Synthesis, Characterization, and Properties of Flexible Magnetic Nanocomposites of Cobalt Ferrite–Polybenzoxazine–Linear Low-Density Polyethylene

Amit B. Rajput,[1] Seikh J. Rahaman,[2] Gautam Sarkhel,[2] Manoj K. Patra,[3] Sampat R. Vadera,[3] Pravin M. Singru,[4] Yusuf Yagci,[5,6] Narendra N. Ghosh[1]

[1]Nano-Materials Lab, Department of Chemistry, Birla Institute of Technology and Science, Pilani KK Birla Goa Campus, Goa 403726, India

[2]Department of Chemical and Polymer Engineering, Birla Institute of Technology, Mesra 835215, Jharkhand, India

[3]Defence Lab, Jodhpur 342011, India

[4]Department of Mechanical Engineering, Birla Institute of Technology and Science, Pilani-KK Birla Goa Campus, Goa 403726, India

[5]Department of Chemistry, Istanbul Technical University, Maslak 34469, Turkey

[6]Chemistry Department, Faculty of Science, King Abdulaziz University, Jeddah, Saudi Arabia

Correspondence to: N. N. Ghosh (E-mail: naren70@yahoo.com)

ABSTRACT: A simple method for the preparation of magnetic nanocomposites consisting of cobalt ferrite (CF; $CoFe_2O_4$) nanoparticles, polybenzoxazine (PB), linear low-density polyethylene (LLDPE), and linear low-density polyethylene-*g*-maleic anhydride (LgM) is described. The composites were prepared by the formation of benzoxazine (BA)–CF nanopowders followed by melt blending with LLDPE and the thermal curing of BA. The composites were characterized by X-ray diffraction, thermogravimetric analysis, differential scanning calorimetry, scanning electron microscopy, universal testing machine measurement, and vibrating sample magnetometry. The composites consisting of LLDPE, PB, and LgM (47.5L–47.5PB–5LgM) exhibited a higher tensile strength (23.82 MPa) than pure LLDPE and a greater elongation at break (6.11%) than pure PB. The tensile strength of the composites decreased from 19.92 to 18.55 MPa with increasing CF loading (from 14.25 to 33.25 wt %). The saturation magnetization of the composites containing 33.25 wt % CF was 18.28 emu/g, and it decreased with decreasing amount of CF in the composite. The composite films exhibited mechanical flexibility and magnetic properties. © 2012 Wiley Periodicals, Inc. J. Appl. Polym. Sci. 128: 3726–3733, 2013

KEYWORDS: composites; magnetism and magnetic properties; mechanical properties; nanoparticles; nanowires and nanocrystals; synthesis and processing

Received 30 April 2012; accepted 2 August 2012; published online 10 October 2012
DOI: 10.1002/app.38426

INTRODUCTION

Recently, magnetic nanocomposites, which are composed of magnetic nanoparticles and polymers, have attracted immense interest because of their light weight and tunable physical properties (e.g., magnetic, electrical, mechanical, and thermal properties).[1,2] These nanocomposites are potential candidates for a plethora of applications, including electronic devices, magnetic data storage, antistatic coatings, rechargeable batteries, and corrosion inhibitors. Ferrites are well-known magnetic materials and possess interesting magnetic and electrical properties.[3]

Ferrite nanoparticles are used in numerous conventional applications, including magnetic recording and storage devices. Some other less traditional but interesting applications include their use as microwave/radar absorbing stealth materials, which are important in defense technology. Although ferrite-based ceramic materials exhibit interesting magnetic and electrical properties along with a high thermal stability, their brittleness and lack of structural flexibility limit their use in complex structured devices. Apart from that, a high sintering temperature (>1200°C) is generally required for the preparation of sintered ferrite bodies. Therefore, it is very difficult to prepare complex structures for specific high-tech applications with pure ferrite nanopowders. A recently active concept for improving the flexibility and processability is based on the hybridization of ceramic materials with organic polymers.

Additional Supporting Information may be found in the online version of this article.

Table I. Compositions of the Prepared Composites

Sample code	LLDPE (wt %)	LgM (wt %)	PB (wt %)	CF (wt %)
BA-CF (70:30)	—	—	70	30
BA-CF (50:50)	—	—	50	50
BA-CF (30:70)	—	—	30	70
47.5L-47.5PB-5LgM	47.5	5	47.5	—
47.5L-5LgM-33.25PB-14.25CF	47.5	5	33.25	14.25
47.5L-5LgM-23.75PB-23.75CF	47.5	5	23.75	23.75
47.5L-5LgM-14.25PB-33.25CF	47.5	5	14.25	33.25

Our objective in this study was to develop ferrite–polymer based nanocomposite sheets and films possessing magnetic properties together with structural flexibility that would be valuable for applications in the manufacture of complex structures or coatings. In this study, we used cobalt ferrite (CF; $CoFe_2O_4$) as the magnetic nanoparticle and a blend of PB and linear low-density polyethylene (LLDPE) as the polymer matrix. PB was deliberately chosen as one of the matrix components in the composites because it offers various advantages, including near-zero shrinkage upon curing, very low water absorption, and good thermal stability.[4] PBs are formed by the thermally activated ring-opening polymerization of the corresponding monomers without the use of any catalysts. PB has the capability of overcoming several shortcomings of conventional novolac- and resole-type phenolic resins. A variety of PB-based composites have been reported in the literature.[5–7] However, PB-based magnetic nanocomposites have scarcely been investigated. Only some studies[8–10] have been concerned with the preparation of PB–magnetic nanocomposites. However, the inherent brittleness of PB needs to be improved if it is to be fabricated into flexible films and used in practical applications for such complex structures. Therefore, in this study, PB was blended with LLDPE because LLDPE possesses excellent low-temperature flexibility, extraordinary processability, better environmental stress cracking resistance, mechanical flexibility, a greater elongation at break, and puncture resistance.[11] In this article, we report the preparation of flexible sheets and films of CF–PB–LLDPE based magnetic nanocomposites with various compositions. The variation in the mechanical and magnetic properties of these composites with changing composition was also investigated.

EXPERIMENTAL

Materials

The chemicals used were $Fe(NO_3)_3{\cdot}9H_2O$, $Co(NO_3)_2{\cdot}6H_2O$, ethylenediamine tetraacetic acid (EDTA; 99.9%, Merck, India), aniline, paraformaldehyde, and bisphenol A (99%, S.D. Fine-Chem, Ltd., India), $CHCl_3$ (99.7%, Qualigens Fine Chemicals, India), LLDPE (R35A042, density = 0.935 g/cm^3, melt flow index = 4.2 g/10 min, GAIL, Ltd. India), and linear low-density polyethylene-*g*-maleic anhydride (LgM; OPTIM E-126, 0.73% maleic anhydride content, melt flow index = 2.16 g/10 min, Pluss Polymers Pvt., Ltd., India). All of the chemicals were used as received.

Synthesis of the CF Nanoparticles

CF nanoparticles, with an average particle size of about 18 nm were synthesized with a simple aqueous-solution-based EDTA precursor developed by us. The detailed synthetic procedure and characterization of CF nanopowders were reported elsewhere.[12] In a typical synthesis, cobalt nitrate, iron(III) nitrate, and EDTA were used as starting compounds. A fluffy, brown-colored precursor was obtained by the reaction of stoichiometric amount of aqueous solutions of metal nitrates with EDTA, followed by evaporation of the reaction mixture to dryness at about 125°C. Calcination of the precursor powder at 550°C for 4 h in air resulted in the formation of CF nanopowders.

Synthesis of the Benzoxazine (BA) Monomer

BA [bis(3-phenyl-3,4-dihydro-2H-1,3-benzoxazinyl) isopropane] was synthesized with a solventless method through the reaction of bisphenol A, aniline, and paraformaldehyde.[13] In a typical synthesis, 4.48 g of bisphenol A, 3.68 mL of aniline, and 2.4 g of paraformaldehyde were mixed in a round-bottom flask and heated slowly at 90°C in an oil bath for 90 min. After cooling, the BA monomer was extracted from reaction mixture by dissolution in $CHCl_3$ followed by filtration. BA monomer was finally obtained through the evaporation of $CHCl_3$. BA monomer was then dried in a vacuum oven for 24 h at 55°C to remove traces of chloroform.

Preparation of BA–CF

For the synthesis of BA–CF, a solvent-casting method was employed. Various compositions of nanocomposites using these powders were prepared by blending with BA and LLDPE, as listed in Table I. BA monomer was dissolved first in chloroform; this was followed by the stepwise addition of CF nanopowder at desired weight ratios. During mixing, the mixture was ultrasonicated. After the completion of mixing, the mixture was dried under reduced pressure in a vacuum oven at 80°C for 12 h. Dynamic light-scattering studies indicated that the average sizes of these BA-coated CF nanoparticles were in the range 100–200 nm. The BA–CF nanocomposite powders thus obtained were used for further composite preparation.

Preparation of the LLDPE–LgM–PB–CF (L–LgM–PB–CF) Nanocomposites

To prepare the CF–PB–LLDPE nanocomposite sheets, BA–CF nanocomposite powders (BA–CF) were blended with LLDPE. LgM was used as a compatibilizer between LLDPE and PB. Nanocomposites having different compositions of CF, PB, and

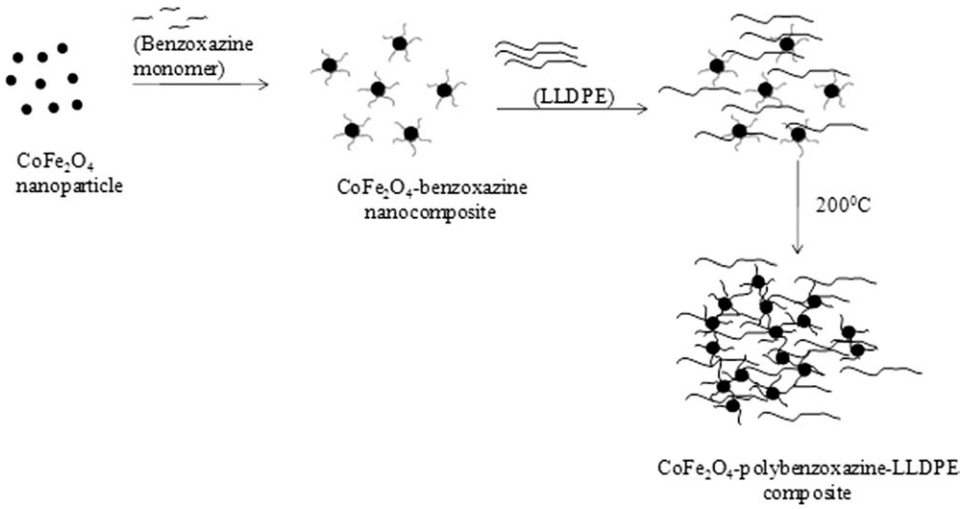

Scheme 1. Schematic diagram of the CF–PB–LLDPE nanocomposite preparation.

LLDPE were prepared, as listed in Table I. The blending of LLDPE, LgM, and BA–CF nanopowders was carried out in a custom-made cylindrical mixing chamber (65 mm in diameter by 65 mm in height) with a two-sided blade stirrer. The temperature of mixing was set at 180°C, and the stirrer speed was 80 rpm. A mixture of LLDPE and LgM was first melted for 10 min; then, BA–CF powder was added and mixed for 20 min. The hot mass was then taken out from the mixing chamber and transferred into a pot and heated at 200°C for 30 min in an oven for the ring-opening polymerization of BA monomer. The hot semiviscous mixture thus obtained was immediately poured into a closed mold under hydraulic pressure through a 5-mm gate. Then material inside the mold cavity was allowed to cool to room temperature, and the mold was opened to obtain the final product. As per the ASTM D 638 standard specification, type-I dog-bone-shaped specimens (with over all dimensions of 165 × 19 × 3.2 mm^3) of the composites were prepared by this method for mechanical testing.

Sample Characterization

Room-temperature X-ray diffraction spectra (XRD) of the calcined powder and cured composites were recorded with a wide-angle powder X-ray diffractometer (Mini Flex II, Rigaku, Japan) with Cu Kα radiation (λ = 0.15405 nm). Thermogravimetric analysis (TGA) and differential scanning calorimetry (DSC) were carried out for the polymer and composites with DTG-60 and DSC-60 instruments (Shimadzu, Japan), respectively. Thermal analyses were performed at a constant heating rate of 10°C/min in an air atmosphere. Tensile measurements were performed according to ASTM D 638 with an Instron 3366 universal testing machine. Type-I dog-bone specimens were tested for the neat PB, LLDPE, and composites. Room-temperature measurements were carried out at a constant crosshead speed of 5 mm/min. The flexural properties of the neat polymers and composite were determined in accordance with ASTM D 790 with an Instron 3366 universal testing machine with a 10-kN load cell. Specimens were tested in a three-point loading with a 50-mm support span at crosshead speed of 5 mm/min at room temperature. The morphology of the fractured surfaces of the composites was studied with scanning electron microscopy (SEM; JSM-6390LV, JEOL, Japan). Room-temperature magnetization measurement was performed for pure CF nanopowder and the composites with a vibrating sample magnetometer (EV5, ADE Technology).

RESULTS AND DISCUSSION

In this study, we combined the useful properties of CF, PB, and LLDPE to prepare flexible magnetic nanocomposites. The method of composite preparation consisted of three steps. Step 1 was the preparation of CF nanoparticles. Step 2 was the mixing of BA monomers with CF nanoparticles, and step 3 was the blending of CF–BA with LLDPE followed by the thermal curing of BA. The overall process is presented in Scheme 1. An SEM micrograph of the surface of a cross section of the composites (Figure 1) showed that PB-coated CF nanoparticles were embedded within the polymeric matrix.

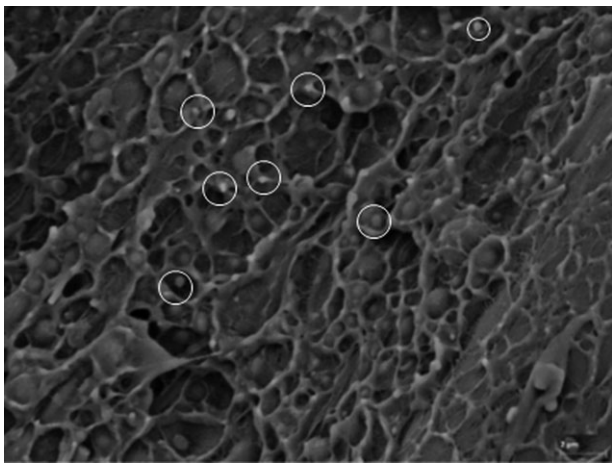

Figure 1. SEM micrograph of the composites showing that the CF nanoparticles were dispersed within the polymeric matrix. The PB-coated CF nanoparticles are marked within the circle.

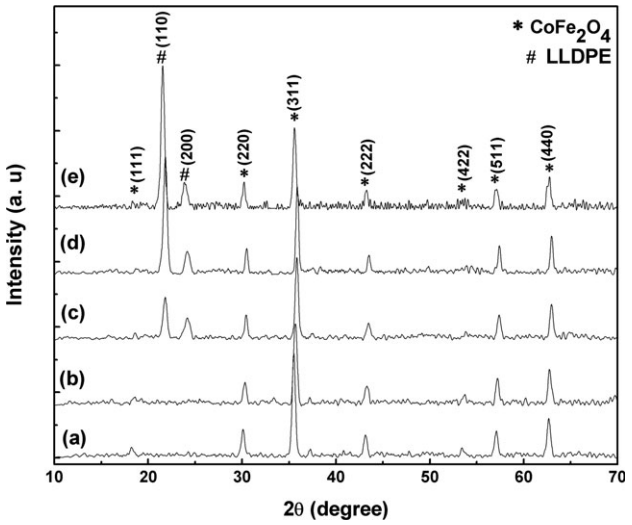

Figure 2. XRD spectra of the (a) CF powder, (b) BA–CF (50:50) nanocomposite, (c) 47.5L–5LgM–33.25PB–14.25CF composite, (d) 47.5L–5LgM–23.75PB–23.75CF composite, and (e) 47.5L–5LgM–14.25PB–33.25CF composite.

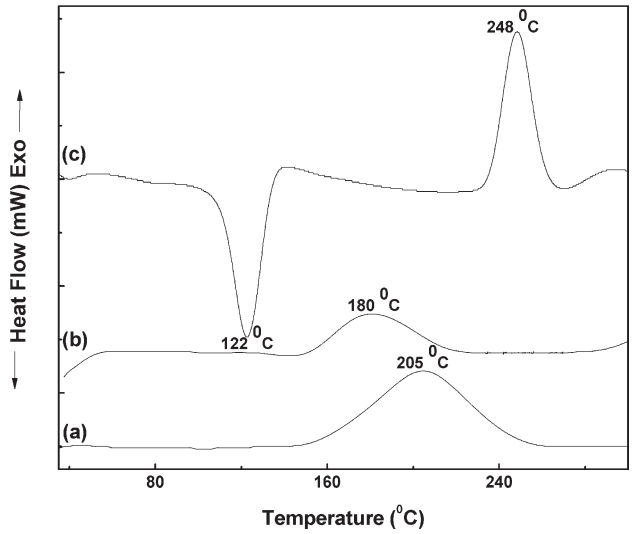

Figure 3. DSC thermogram of the (a) BA monomer, (b) BA–CF (50:50) nanocomposite, and (c) 47.5L–5LgM–23.75PB–23.75CF composite.

XRD Analysis

XRD spectra were recorded for the pure CF nanopowders, BA–CF nanocomposites, and L–LgM–PB–CF composites. In the XRD spectra of the pure CF nanopowder, the presence of peaks corresponding to (111), (220), (311), (222), (400), (422), (511), and (440) diffraction planes confirmed the formation of single-phase CF [Figure 2(a)].[12] In case of the BA–CF nanocomposite samples, all XRD peaks of CF were present, and no additional peaks were detected [Figure 2(b)]. In the XRD spectra of the L–LgM–PB–CF nanocomposite samples, XRD peaks of CF were present along with additional peaks at $2\theta = 21.6$ and 23.8°. These two peaks corresponded to the (110) and (200) diffraction planes of LLDPE[14] and indicated that the crystalline structure of LLDPE remained unchanged on blending in the nanocomposites. However, the intensity of the crystalline peaks of LLDPE varied with the compositions. These XRD spectra of the composites also confirmed that the pure crystalline phase of CF remained preserved in the composite with no impurity phase formation during the melt-blending process.

Thermal Analysis

TGA and DSC of the pure BA, BA–CF, and L–LgM–PB–CF composites were performed to evaluate the thermal stability. In the DSC thermogram of the BA monomer, an exothermic peak at 205°C was observed, which was due to ring-opening polymerization of the BA ring [Figure 3(a)].[5,9] In case of BA–CF, this exothermic curing peak of BA shifted to a lower temperature of 180°C. This might have been due to the catalytic effect of CF toward the thermal curing of BA [Figure 3(b)]. For the L–LgM–PB–CF composite samples, an endothermic peak at 122°C, corresponding to the melting temperature of LLDPE, was observed.[14] However, the exothermic peak for the ring-opening polymerization of the BA ring was absent in this thermogram [Figure 3(c)]. This result indicates that all of the BA monomer was fully polymerized to PB during composite preparation when the melt blending was performed at 200°C. An exothermic peak at 248°C was observed; this was due to the thermal degradation of the polymer component of the composite.

From the TGA of pure PB, LLDPE, and their composites, the temperature at 5% weight loss ($T_{5\%}$), temperature at 10% weight loss ($T_{10\%}$), and char yield (%) at 800°C in air were determined and are listed in Table II. TGA thermograms of the LLDPE, PB, BA–CF, and L–LgM–PB–CF nanocomposite are shown in Figure 4. These thermograms revealed that the presence of a more thermally stable PB in the L–LgM–PB–CF composites enhanced the overall thermal stability of the composites. However, as the melting temperature of LLDPE was 122°C, the composites should be used below this temperature.

Mechanical Properties and SEM Analysis

To evaluate the mechanical properties of the prepared L–LgM–PB–CF composites, tensile tests and three-point bending flexural tests were performed. The tensile stress–strain curves of the PB, LLDPE, 47.5L–47.5PB–5LgM blend, and L–LgM–PB–CF

Table II. Thermal Degradation Properties of the Composites

Sample code	$T_{5\%}$ (°C)	$T_{10\%}$ (°C)	Char yield (%) at 800°C
PB	350	400	0
LLDPE	267	305	0
PB-CF (70:30)	301	375	25
PB-CF (50:50)	270	364	46
PB-CF (30:70)	265	362	63
47.5L-5LgM-33.25PB-14.25CF	316	365	15
47.5L-5LgM-23.75PB-23.75CF	310	354	20
47.5L-5LgM-14.25PB-33.25CF	288	343	30

Applied Polymer SCIENCE

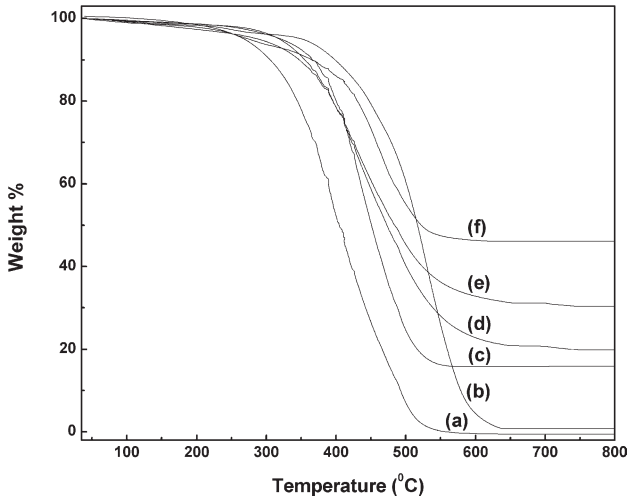

Figure 4. TGA thermograms of (a) LLDPE, (b) PB, (c) 47.5L–5LgM–33.25PB–14.25CF composite, (d) 47.5L–5LgM–23.75PB–23.75CF composite, (e) 47.5L–5LgM–14.25PB–33.25CF composite, and (f) PB–CF (50:50) nanocomposite.

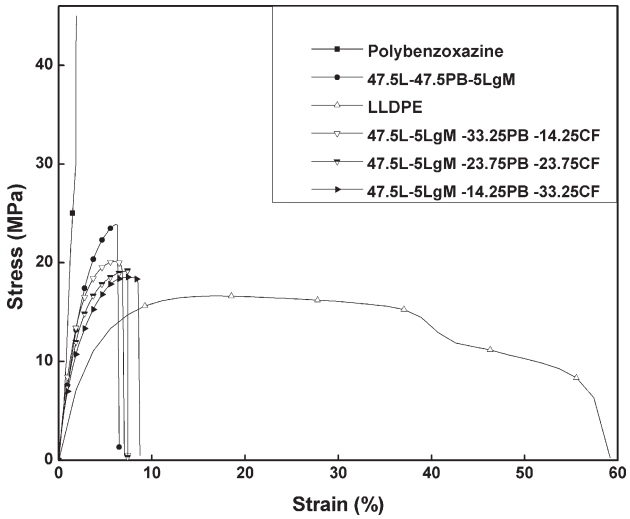

Figure 5. Tensile stress–strain curves of the composites.

composite are shown in Figure 5. The morphology of the fractured surface of the samples were also investigated by SEM (Figure 6).

It was observed that whereas pure PB possessed a high tensile strength (45 MPa) and lower elongation at break (2.2%), LLDPE showed a low tensile strength (16.6 MPa) and a significantly greater elongation at break (57%). The composites consisted of LLDPE and PB with 5 wt % compatibilizer LgM (47.5L–47.5PB–5LgM) and exhibited a higher tensile strength

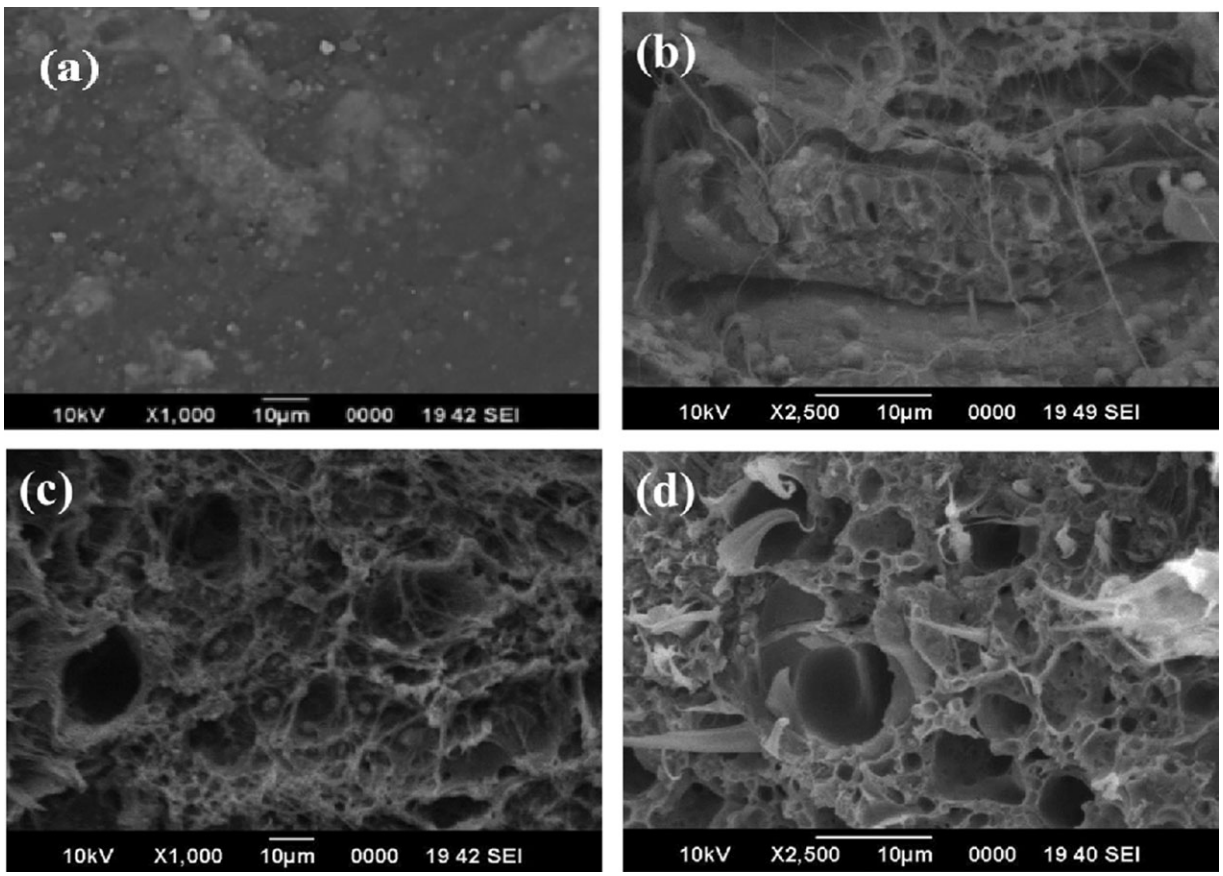

Figure 6. SEM micrographs of the (a) surface of the 47.5L–5LgM–23.75PB–23.75CF composite before tensile testing and fractured surfaces of composites after tensile testing, (b) 47.5L–5LgM–33.25PB–14.25CF, (c) 47.5L–5LgM–23.75PB–23.75CF, and (d) 47.5L–5LgM–14.25PB–33.25CF.

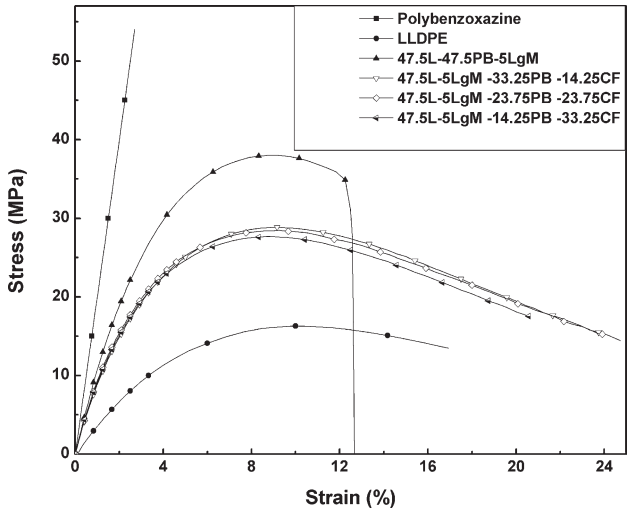

Figure 7. Flexural stress–strain curves of the neat polymer, blend, and L–LgM–PB–CF composite.

(23.82 MPa) than pure LLDPE and a greater elongation at break (6.11%) than pure PB. This might have been due to the binding role of the compatibilizer (LgM), which enhanced the chemical and physical interaction among the two separate phases (i.e., PB and LLDPE)[15] and ultimately improved their interfacial adhesion by reducing the interfacial tension. The SEM micrograph of the composite [Figure 6(a)] showed the homogeneous polymeric matrix of the composite and no phase separation between PB and LLDPE in the presence of the LgM compatibilizer.

The incorporation of CF nanoparticles in the L–LgM–PB–CF composites resulted in a decrease in the tensile strength of the composites compared to that of 47.5L–47.5PB–5LgM blend (23.82 MPa). The tensile strength decreased slightly (from 19.92 to 18.55 MPa) with increasing CF loading (from 14.25 to 33.25 wt %) in the composition. This might have been due to the higher particle loading, which resulted in the agglomeration of the particles, which caused an increase in the interfacial tension. Therefore, loading stress was not easily transferred from the polymer matrix to the particles, and ultimately, the tensile strength of the L–LgM–PB–CF composites decreased with increasing CF amount.[16–19] The elongation at break of the composites also decreased with increasing amount of CF nanoparticles in the composite composition. The morphology of the fractured surfaces of the composites after tensile testing was investigated by SEM and is shown in Figure 6(b–d). We observed that delamination of the nanoparticles from the polymeric matrix occurred under tensile strain and the formation of voids during breaking. This effect was pronounced for the composites having larger CF loadings, and large voids were observed in their fractured surfaces [Figure 6(c, d)]. This might have been the cause of the decrease in the tensile properties of the composites with increasing CF loading.

However, the tensile strengths of the composites were found to be higher than that of pure LLDPE. From the flexural stress–strain curves (Figure 7) of the PB, LLDPE, 47.5L–47.5PB–5LgM blend, and L–LgM–PB–CF composites, we observed that the L–LgM–PB–CF composites possessed a higher flexural strength than that of pure LLDPE but a lower flexural strength than that of the 47.5L–47.5PB–5LgM blend. However, the toughness (area under the stress–strain curve) of the L–LgM–PB–CF composites was higher than those of the neat PB, neat LLDPE, and 47.5L–47.5PB–5LgM blend. The mechanical properties of the neat polymers and composites are summarized in Table III.

Magnetic Properties

The variation of magnetic properties, in terms of saturation magnetization (M_s) and coercivity (H_c), with the composition of composites were investigated with a vibrating sample magnetometer at room temperature with an applied field of 15,000 Oe. Figure 8 shows the hysteresis loops obtained for the pure CF nanoparticles, BA–CF, and the series of L–LgM–PB–CF composites, and the values of M_s and H_c are summarized in Table IV. M_s and H_c values of CF nanoparticles were 67.55 emu/g and 1645.24 Oe, respectively. We observed that when the CF nanoparticles were mixed with BA (BA–CF samples), the M_s value of the samples decreased. In the L–LgM–PB–CF composites, the same trend was also observed. This decrease in the M_s value with decreasing CF amount in the composite was quite obvious because the composite was composed of magnetic CF nanoparticles and a nonmagnetic polymer. The H_c value of the composite was found to be higher than that of the pure CF nanoparticles. This might have been due to the increased interparticle distance in the composite as compared to the close contact of the pure nanoparticles.[20–22]

Figure 9 demonstrates that a film of the L–LgM–PB–CF composite was attached with a bar magnet, which indicated its magnetic nature. Both ends of the film could be gripped by tweezers and easily bended because of its mechanical flexibility. This

Table III. Tensile and Flexural Properties of the Composites

Sample code	Tensile strength (MPa)	Tensile modulus (GPa)	Elongation at break (%)	Flexural strength (MPa)	Flexural modulus (GPa)	Toughness (MPa)
LLDPE	16.60	0.236	57	16.33	0.403	0.274
PB	45.17	3.6	2.2	54.06	1.928	0.439
47.5L-47.5PB-5LgM	23.82	0.982	6.11	38.01	1.240	0.244
47.5L-5LgM-33.25PB-14.25CF	19.92	1.110	8.7	28.70	1.184	0.535
47.5L-5LgM-23.75PB-23.75CF	19.16	0.981	7.4	28.43	1.126	0.524
47.5L-5LgM-14.25PB-33.25CF	18.55	0.973	6.11	27.67	1.102	0.479

Applied Polymer SCIENCE

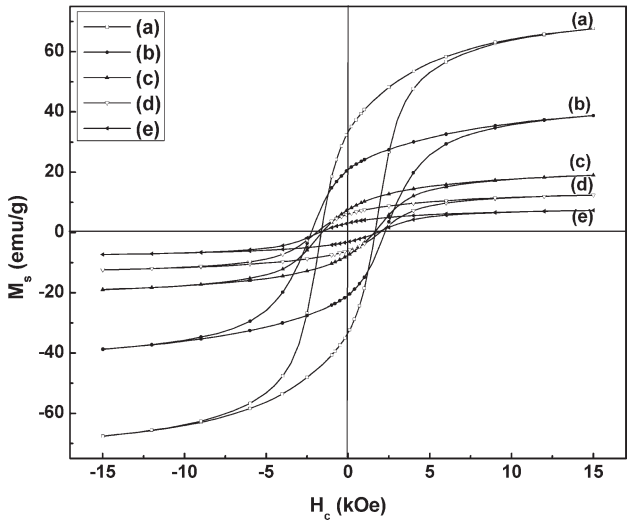

Figure 8. Magnetization curves for the (a) CF powder, (b) PB–CF (50:50) nanocomposite, (c) 47.5L–5LgM–14.25PB–33.25CF, (d) 47.5L–5LgM–23.75PB–23.75CF, and (e) 47.5L–5LgM–33.25PB–14.25CF.

shows that the composites reported here possess magnetic properties along with mechanical flexibility.

CONCLUSIONS

We prepared nanocomposites composed of CF nanoparticles, PB, and LLDPE. XRD analysis showed that spinel phase of CF was present in the cured composites. The mechanical properties of the composites were assessed with tensile and flexural testing. Tensile testing of the samples revealed that pure PB possessed a higher tensile strength and lower elongation at break compared to LLDPE. The composite consisting of LLDPE, PB, and 5 wt % LgM compatibilizer exhibited a higher tensile strength than pure LLDPE and a greater elongation at break than pure PB. An increase in the CF loading in the composites resulted in a decrease in the tensile properties of the composites. The L–LgM–PB–CF composites possessed a higher flexural strength than that of pure LLDPE but a lower flexural strength than 47.5L–47.5PB–5LgM. However, the toughness of the L–LgM–PB–CF composites was higher than that of the pure PB, pure LLDPE, and 47.5L–47.5PB–5LgM blend. The incorporation of CF nanoparticles introduced magnetic properties to the composites, and composites having 33.25 wt % CF nanoparticles possessed an M_s of 18.9 emu/g and an H_c of 1931 Oe.

Table IV. Magnetic Properties of the Composites

Sample code	M_s (emu/g)	H_c (Oe)
CF	67.55	1645.23
PB–CF (70:30)	16.53	2056.16
PB–CF (50:50)	27.57	2134.84
PB–CF (30:70)	38.80	2243.51
47.5L–5LgM–14.25PB–33.25CF	18.9	1931.95
47.5L–5LgM–23.75PB–23.75CF	12.4	1595.82
47.5L–5LgM–33.25PB–14.25CF	7.24	1753.62

The method of preparation of the composites reported here is very simple and does not require any elaborate set up. The mechanical and magnetic properties of these composites could be tailored by the judicious choice of compositions. As the sheets and films of these composites showed structural flexibility and magnetic properties, these composites have the

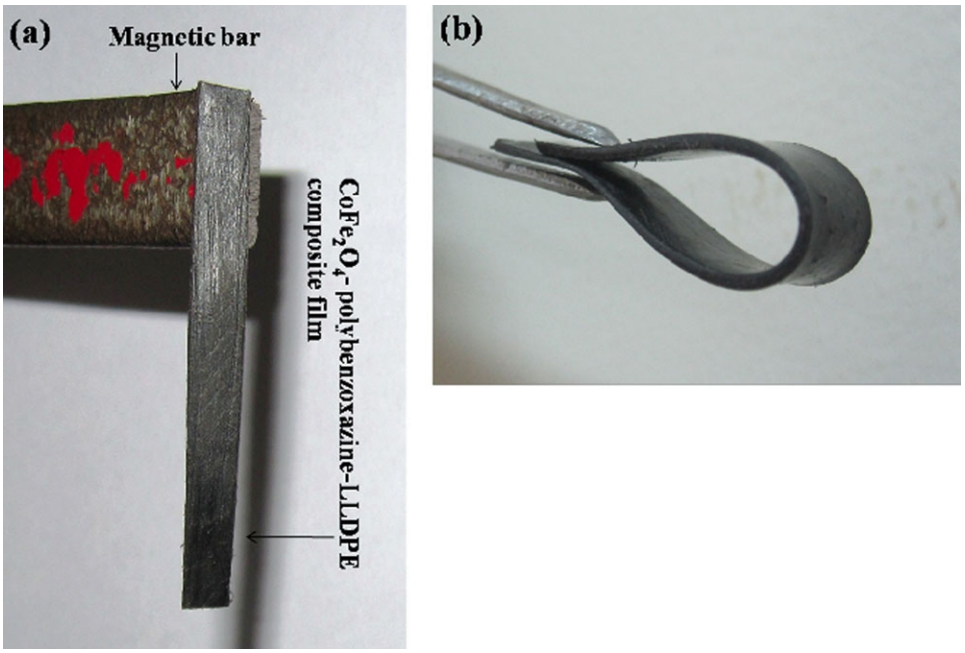

Figure 9. CF–PB–LLDPE composite film exhibiting its (a) magnetic nature and (b) mechanical flexibility. [Color figure can be viewed in the online issue, which is available at wileyonlinelibrary.com.]

capability of being used in complex device applications and coatings.

ACKNOWLEDGMENTS

One of the authors (N.N.G.) gratefully acknowledges the financial support from Defence Research & Development Organisation (DRDO) (contract grant number ERIP/ER/0904500/M/01/1204).

REFERENCES

1. Morais, P. C.; Oliveira, A. C.; Garg, V. K.; Silva, M. L.; Alcântara, E. F. C.; Soares, F. Q.; Rabelo, D. *Hyperfine Interact.* **2007**, *179*, 51.
2. Jiang, J.; Ai, L.; Li, L. C. *J. Mater. Sci.* **2009**, *44*, 1024.
3. Pant, P.; Bhuvaneswari, S.; Ghosh, N. N. *Recent Pat. Nanotechnol.* **2008**, *2*, 8.
4. Handbook of Polybenzoxazine Resin; Ishida, H., Agag, T., Eds.; Elsevier: Amsterdam, **2011**.
5. Ghosh, N. N.; Kiskan, B.; Yagci, Y. *Prog. Polym. Sci.* **2007**, *32*, 1344.
6. Yagci, Y.; Kiskan, B.; Ghosh, N. N. *J. Polym. Sci. Part A: Polym. Chem.* **2009**, *47*, 5565.
7. Kiskan, B.; Ghosh, N. N.; Yagci, Y. *Polym. Int.* **2011**, *60*, 167.
8. Ghosh, N. N.; Rajput, A. B. In Handbook of Polybenzoxazine Resins; Ishida, H.; Agag, T., Eds.; Elsevier: Amsterdam, **2011**; Chapter 37, p 641.
9. Sarangi, P. P.; Naik, B.; Vadera, S. R.; Patra, M. K.; Prakash, C.; Ghosh, N. N. *Mater. Technol.* **2010**, *25*, 271.
10. Kiskan, B.; Demirel, L.; Kamer, O.; Yagci, Y. *J. Polym. Sci. Part A: Polym. Chem.* **2008**, *46*, 6780.
11. Bhadrakumari, S.; Predeep, P. *J. Supercond. Nov. Magn.* **2008**, *21*, 313.
12. Rajput, A. B.; Hazra, S.; Ghosh, N. N. *J. Exp. Nanosci.* DOI: 10.1080/17458080.2011.582170. Published Online: May 3, 2012. http://www.tandfonline.com/doi/full/10.1080/17458080.2011.582170.
13. Brunovska, Z.; Liu, J. P.; Ishida, H. *Macromol. Chem. Phys.* **1999**, *200*, 1745.
14. Borah, J. S.; Chaki, T. K. *J. Polym. Res.* **2011**, *18*, 569.
15. Borah, J. S.; Chaki, T. K. *J. Polym. Res.* **2011**, *18*, 907.
16. Jeon, I.; Baek, J. *Materials* **2010**, *3*, 3654.
17. Guo, Z. H.; Liang, X. F.; Pereira, T.; Scaffaro, R.; Hahn, H. T. *Compos. Sci. Technol.* **2007**, *67*, 2036.
18. Guo, Z. H.; Lei, K.; Li, Y. T.; Ng, H. W.; Prikhodko, S.; Hahn, H. T. *Compos. Sci. Technol.* **2008**, *68*, 1513.
19. Fu, S. Y.; Feng, X. Q.; Lauke, B.; Mai, Y. W. *Compos. B* **2008**, *39*, 933.
20. Guo, Z. H.; Park, S.; Wei, S. Y.; Pereira, T.; Moldovan, M.; Karki, A. B.; Young, D. P.; Hahn, H. T. *Nanotechnology* **2007**, *18*, 335704.
21. Zhang, D.; Klabunde, K. J.; Sorensen, C. M.; Hadjipanayis, G. C. *Phys. Rev. B* **1998**, *58*, 14167.
22. Sorensen, C. M. In Nanoscale Materials in Chemistry; Klabunde, K. J., Ed.; Wiley-Interscience: New York, **2001**; Chapter 6, p 169.